

1
2
3
4
5
6
7
8
9
10
11
12
13
14
15
16
17
18
19
20
21
22

Climate change will increase savannas at the expense of forests and treeless vegetation in tropical and subtropical Americas

José D. Anadón^{1,2}, Osvaldo E. Sala^{1,3*} and Fernando T. Maestre⁴

¹ School of Life Sciences and School of Sustainability, Arizona State University, Tempe, AZ 85287, USA

² Department of Biology, Queens College, City University of New York, Flushing, NY 11367, USA

³ South American Institute for Resilience and Sustainability Studies, SARAS², Maldonado, Uruguay

⁴ Departamento de Biología y Geología, Escuela Superior de Ciencias Experimentales y Tecnología, Universidad Rey Juan Carlos, Móstoles, 28933, Spain

*Correspondence author:

Running title: Climate Change and vegetation transitions

Key-words: climate change impacts, forest, plant–climate interactions, savanna, treeless vegetation, vegetation transitions

23 **SUMMARY**

24
25
26
27
28
29
30
31
32
33
34
35
36
37
38
39
40
41
42
43
44
45
46
47
48
49
50

1. Transition areas between biomes are particularly sensitive to environmental changes. Our understanding of the impacts of ongoing climate change on terrestrial ecosystems has significantly increased during the last years. However, it is largely unknown how climatic change will affect transitions among major vegetation types.

2. We modeled the distribution of three alternative states (forest, savanna and treeless areas) in the tropical and subtropical Americas by means of climate-niche modeling. We studied how such distribution will change by the year 2070 by using 17 downscaled and calibrated global-climate models from the Coupled Model Intercomparison Project Phase 5 and the latest scenarios provided by the 5th Assessment Report of the IPCC.

3. Our results support the savannization of the tropical and subtropical Americas because of climate change, with an increase of savannas mainly at the expense of forests.

4. Our models predict an important geographical shift in the current distribution of transition areas between forest and savannas, which is much less pronounced in the case of those between savannas and treeless areas. Largest shifts, up to 600 km northward, are predicted in the forest-savanna transitions located in the eastern Amazon.

5. Our findings indicate that climate change will promote a shift towards more unstable states: the extent of the transition areas will notably increase, and largely stable forest areas are predicted to shrink dramatically.

6. *Synthesis.* Our work explores dimensions of the impact of climate change on biomes that have received little attention so far. Our results indicate that climate change will not only affect the extent of savanna, forest and treeless areas in the tropical and subtropical Americas, but also will: i) promote a significant geographical shift and an increase of the extent of transition areas between biomes, and ii) decrease the stability of the equilibrium between forest, savanna and treeless areas, yielding a more unpredictable system.

51 **INTRODUCTION**

52 The Fifth Assessment Report of the Intergovernmental Panel on Climate Change (IPCC)
53 provides unequivocal evidence of ongoing climate change, which is characterized by an increase
54 in temperature globally and important modifications in rainfall patterns (IPCC, 2013). Climate
55 change will have major impacts on the structure and functioning of terrestrial ecosystems
56 (Peñuelas *et al.*, 2013), and is already promoting important changes in the spatial extent and
57 distribution of vegetation types worldwide (Gang *et al.*, 2013). Our understanding of the impacts
58 of ongoing climate change on terrestrial ecosystems has significantly increased in recent years
59 (see Parmesan (2006); Parmesan & Yohe (2003); Paruelo *et al.* (1995); Walther (2010) and
60 Peñuelas *et al.* (2013) for reviews). In tropical areas, forests might retreat yielding more open
61 savanna-like systems, a pattern particularly well identified for the Amazonian region (Franchito,
62 Rao & Fernandez, 2012; Salazar, Nobre & Oyama, 2007; Zelazowski *et al.*, 2011).
63 Climate-induced changes in vegetation types will have direct effects on the provisioning of
64 ecosystem services for humans (MEA, 2003). Shifts from grasslands into woodlands results in a
65 significant reduction in livestock production (Anadón *et al.*, 2014), which can be offset by an
66 increase in carbon sequestration (Havstad *et al.*, 2007) and soil fertility (Eldridge *et al.*, 2011).
67 The shift from forest to grassland can also have impacts on ecosystem services other than the
68 provisioning of timber or food, **such as a decrease in carbon sequestration and regulation of**
69 **climate** (MEA, 2003).

70 Biome transitions are areas of high socio-ecological interest for many reasons. These
71 areas have a unique and high biological diversity at multiple levels (from genes to communities;
72 see Kark & Van Rensburg (2006) for a review), and are areas of high conservation interest
73 (Smith *et al.*, 2001; Smith *et al.*, 1997). These areas are also particularly sensitive to human

74 activities such as grazing (Hudak, 1999), and to important components of climate change such as
75 the increase in precipitation intensity and rainfall variability predicted for many terrestrial
76 ecosystems worldwide (IPCC, 2013; Meehl, Arblaster & Tebaldi, 2005). In this direction, rapid
77 vegetation shifts in responses to recent changes in climatic conditions are already being detected
78 in areas such as the Arctic tundra (Sturm, Racine & Tape, 2001), the Alps (Gehrig-Fasel, Guisan
79 & Zimmermann, 2007) and the drylands of the Southwestern U.S. (Van Auken, 2009). Recent
80 studies have highlighted how climate change drivers, such as an intensification of the rainfall
81 regime, may favor the recruitment and expansion of woody plants in savannah ecosystems
82 (Holmgren et al., 2013; Kulmatiski & Beard, 2013), a vegetation transition with major ecological
83 effects on biodiversity, nutrient cycling and carbon sequestration in drylands worldwide
84 (Eldridge et al., 2011). **As such, forecasting how vegetation in transitional areas will respond to
85 climate change is an urgent ecological question that has been poorly studied to date.**

86 Understanding how climatic variables such as rainfall and temperature determine woody
87 vegetation cover in grassland-woodland transition areas has been an area of active research in the
88 last decades (Hirota et al., 2011; Sankaran et al., 2005; Staver, Archibald & Levin, 2011;
89 Williams et al., 1996). Continental-scale analyses of tree cover in African savannas have found
90 that mean annual precipitation largely limits the maximum cover of woody species, and that
91 disturbance dynamics control savanna structure below this maximum (Sankaran et al., 2005).
92 More recent analyses have reported the presence of three alternative stable states (forest,
93 savanna, and treeless) in the world's savannas (Hirota et al., 2011). These authors found that the
94 tree cover values characterizing savannas (~20%) and forests (~80%) were found over multiple
95 rainfall conditions, suggesting that woody cover is not controlled by gradual increases in
96 precipitation, and that there is a shifting probability of being in either of the three stable states

97 identified. The reverse side of this multiple stable state equilibrium is the existence of highly
98 unstable tree cover values (~5% and ~60%) that can be then identified as transition areas
99 between biomes. A key property of the findings reported by Hirota *et al.* (2011) is that any given
100 locality will have a probability of being forest, savanna and desert according to their climatic
101 characteristics, and thus they allow us to quantify how likely transitions between vegetation
102 types are likely to occur. For example, in a locality with very high probability of being forest and
103 low of being savanna or treeless, the probability of transition between vegetation states is very
104 low. As a consequence, the uncertainty of the locality is very low since it is highly probable that
105 it will be a forest. On the contrary, the uncertainty of a locality with similar and high
106 probabilities of being forest and savanna (and low probability of being treeless) is very high,
107 since it is very difficult to predict whether this locality will be a forest or a savanna. In localities
108 of high uncertainty, small changes in tree cover due to human activities (e.g. fires, selective
109 logging) might have a large effect on the system and promote the transition from one state to
110 another. On the contrary, localities with low uncertainty are likely to be more resilient to human-
111 induced changes to tree cover (Hirota et al., 2011).

112 While research conducted over the last decades has provided key insights to advance our
113 understanding of the mechanisms driving grass/woody vegetation coexistence in savanna
114 systems, and has improve our ability to predict their responses to climate change, no previous
115 studies so far have explicitly evaluated how forest-savanna-treeless transitions will change under
116 future climatic conditions at regional to continental scales (but see Hutyrá et al. (2005); Salazar,
117 Nobre & Oyama (2007); Salazar & Nobre (2010) for forest-savanna transitions). We aimed to
118 assess forest-savanna-treeless transitions under climate change for the tropical and subtropical
119 Americas; a region that is crucial for preserving global biodiversity (Myers et al., 2000),

120 regulating the Earth's climate (Gedney & Valdes, 2000), and that directly supports the livelihood
121 of more than 700 million people. Our objectives were to: i) assess the climatic determinants of
122 the occurrence of treeless vegetation, savannas and forest in the tropical and subtropical
123 Americas, ii) predict the future extent and distribution under climate change scenarios of treeless
124 vegetation, savannas and forest in that region, iii) evaluate how climate change will affect the
125 distribution of the transition areas among them, and iv) assess how climate change will affect the
126 uncertainty of the occurrence of different vegetation types. To achieve these objectives, we
127 modeled the spatial distribution of grasslands and woodlands and their transition areas in the
128 studied region using the alternative stable state framework provided by Hirota et al. (2011) and
129 large-scale remote sensing and climate data, and employed the latest climate change scenarios
130 provided by the 5th Assessment Report of the IPCC (Taylor, Stouffer & Meehl, 2012) to forecast
131 how such distribution will change by the year 2070.

132

133 **MATERIALS AND METHODS**

134 **Modeling the distribution of forest, savanna and treeless areas**

135 Our study area comprises the tropical and subtropical Americas, here defined as those areas
136 between latitude 35°N and 35°S. Hirota *et al.* (2011) suggested that the different vegetation types
137 in tropical areas, as described by tree cover, are actually alternative states, exhibiting sharp
138 transitions between them at so-called tipping points. These authors identified three alternative
139 states in the tropical areas of the Americas (forest, savanna and treeless areas) that were defined
140 by the cutting levels of 5 and 60% of tree cover (i.e., treeless=0-5%, savanna=5-60%, forest=60-
141 100%).

142 We modeled the distribution of the three states (forest, savanna or treeless) according to climatic
143 variables by means of generalized linear models with a binomial distribution of errors, with the
144 presence/absence of the state as independent variables, and with climatic descriptors (Mean
145 annual temperature [T], Mean annual precipitation [P], T + P, P/T ratio and Aridity index
146 [P/Potential evapotranspiration]) as independent variables. **Our models rely on the understanding
147 that climate governs the broadest outlines of distributions of species and biomes. This statement
148 is well supported by current knowledge (see Araújo & Peterson (2012) for a review). In this
149 sense, our models capture the main controls of biome distribution at a continental scale (i.e.,
150 climate), as shown by the high values of explained deviance obtained (see Results section).**
151 Models were fitted to a random sample of 3000 2.5' x 2.5' (aprox. 4.5 x 4.5 km) cells from the
152 study area. Tree cover percentage was assessed from the MOD44B Collection 3 product from
153 MODIS (Hansen et al., 2003) originally at a 500 m resolution. 2.5 arc-minute resolution values
154 were obtained by averaging the 500 m side cells within each 2.5 arc-minute side cell. Average
155 tree-cover values were then transformed to a categorical map describing the three alternative
156 states in the present time, using the 5% and 60% cutting levels described above. Mean annual
157 precipitation, temperature and evapotranspiration were also assessed for each 2.5 arc-minute side
158 cell. Precipitation and temperature were obtained from Worldclim database
159 (www.worldclim.org; Hijmans et al. 2005). Evapotranspiration was obtained from the Global
160 Potential Evapo-Transpiration (Global-PET) dataset (<http://www.cgiar-csi.org/>). Both databases
161 describe climatic average values of the period 1950-2000 and are available at a 2.5 arc-minute
162 resolution.

163 Eleven candidate models were fitted to the MOD44B data, including linear and quadratic
164 responses to the different climatic descriptors (Table 1). Models for each state were ranked

165 according to the Akaike Information criterion (Burnham & Anderson, 2002). In accordance with
166 previous works showing that tree cover and climate relationships at the continental scale are
167 insensitive to the spatial resolution (Staver, Archibald & Levin, 2011), our results at 2.5 arc-
168 minutes resolution were very similar to those obtained using a 30 second (aprox. 1 km)
169 resolution (data not shown). We used the Global Land Cover 2000 (GLC2000) map to filter out
170 areas undergoing human activities (categories 16-18 and 22; (Bartholome & Belward, 2005)
171 from our analyses. **These areas cover $5.1 \times 10^6 \text{ km}^2$, comprising 23% of our study area (Fig. S1).**
172 By only using natural areas, we maximize the decoupling of climate and land-use controls on the
173 dynamics of biomes and their transitions areas. As such, our predictions are based solely on
174 climatic controls and are largely independent of land-use change.

175 As it will be detailed in the Results section, a global model (i.e. including all the study
176 area) for forest and treeless states presented high explanatory power ($D^2 > 40\%$; Table 1). For the
177 savanna state, however, the best global model according to the Akaike Information criterion
178 performed poorly ($D^2 = 12\%$; Table 1), suggesting spatial non-stationarity (i.e. the response of the
179 savanna state to climatic condition changes within our study area). To obtain a more robust
180 model, and starting from the best global model ($P^2 + T^2$; Table 1), we developed models with a
181 spatial factor describing different subareas within our study area. This factor was included as an
182 interaction term in the models. Because of the latitudinal organization of macroclimatic control
183 and major biomes on the Earth (Bailey & Ropes, 1998), this factor divided our study area
184 latitudinally in two or three areas. Since we did not know which areas were a priori responsible
185 for the presence of non-stationarity in our data, we fitted models with different spatial factors
186 describing all possible two and three latitudinal subareas within our study area. To make the
187 number of latitudinal subareas tractable, the minimum latitudinal width of the subareas were 5°

188 (for example from 15°N to 20°N, see Table S1 in Supporting Information for examples of factors
189 including different latitudinal subareas). In total we fitted 91 models, each one including the best
190 global model and a spatial factor. As detailed in the Results section below, a large number of
191 models had a very similar explanatory power (Table S1, Supplementary Information). Hence, the
192 model for the savanna state was built using a weighted average consensus approach (Marmion et
193 al., 2009). For doing so, we first selected a subset of models with the highest accuracy, and then
194 calculated a weighted average according to a model performance metric (Hartley, Harris &
195 Lester, 2006; Marmion et al., 2009). In our case, and given the differences in the explanatory
196 power of the models, we selected the 20% best models according to their explained variance ($n =$
197 18 models, range of explained variance of these models = 27.6-33.6%). Models were weighted
198 according also to their explained deviance (Araujo et al. 2007). We did not use the Akaike
199 weights (Burnham & Anderson, 2002) for model averaging because this approach led us to the
200 selection of only one best model (i.e. weight of the first ranked model = 0.996).

201 Our distribution models for forest, savanna and treeless areas were projected to the study
202 area using present conditions (1950-2000) and climate change scenarios. For the scenarios, we
203 used 17 downscaled and calibrated global climate models from the Coupled Model
204 Intercomparison Project Phase 5 (CMIP5) (Taylor, Stouffer & Meehl, 2012) (See Table S2,
205 Supplementary Information). We selected for our projections the Representative Concentration
206 Pathway 8.5 (RCP8.5) for the year 2070. Within the Fifth IPCC Assessment Report, RCP8.5
207 represents the scenario with the highest concentration of greenhouse gases, and with a predictive
208 radiative forcing of $+ 8.5\text{W/m}^2$ (IPCC, 2013). Our rationale behind the selection of the worst (but
209 possible) scenario is that we are more interested in capturing the overall directions of the changes
210 than in quantifying exactly the extent of the changes. To describe the extent of forest, savanna

211 and treeless areas in the present time and for the year 2070, each cell was assigned to the state
212 with largest probability of occurrence.

213

214 **Modeling transitions**

215 Our study system is comprised by three states (forest, savanna and treeless areas) and two
216 possible transitions (forest-savanna and savanna-treeless). To model these two transitions, we
217 first divided our study area in the forest-savanna and savanna-treeless systems. These two
218 subareas are mutually exclusive. The forest-savanna system is defined as those areas where the
219 probability in the present time of being savanna or forest is larger than the probability of being
220 treeless. Conversely, the savanna-treeless system is defined as those areas where the probability
221 of being savanna or treeless in the present time is larger than the probability of being forest (Figs.
222 2 and 3). Starting from the distribution maps of the three alternative states for the present time
223 and the climate-change scenario of the 17 CMIP5 global climate models, we calculated transition
224 maps between forest and savanna, and between savanna and treeless areas for these two periods.
225 In the transition maps, we calculated for each cell a transition index ($Trans_{AB}$) calculated as
226 $Trans_{AB} = p(A) - P(B)$, where $P(A)$ and $P(B)$ are the probability of being in state A and B, as
227 described by the distribution maps. The transition index ranges between 1 and -1, with 1 being
228 those cells with the largest probability of being in state A and least probability of being in state
229 B, and -1 the other way around (maximum probability of being in state B and least of being in
230 state A). Values close to 0 indicate high uncertainty, being difficult to predict whether the cell
231 will be in state A or B, and cells with $Trans_{AB}=0$ are those that have exactly the same probability
232 of being in state A or B, according to their climatic conditions. From the transition maps we
233 identified transition areas, i.e. areas with the highest uncertainty, which were defined as those

234 with $Trans_{AB}$ absolute values below 0.2. In the same vein, we defined the core areas of the
235 biomes, i.e. areas with the lowest uncertainty, as those with $Trans_{AB}$ absolute values above 0.5.
236 The modeling approach described above was performed for each one of the 17 CMIP5 global
237 climate models. Final projection maps for biome distribution, transition areas and their changes
238 were built from the ensemble mean of the projections provided by the 17 models (Araújo &
239 New, 2007).

240

241 RESULTS

242 For the three states considered, the models with the largest values of explained deviance were
243 those including temperature and precipitation (Table 1). The best models for forests and
244 savannas included both variables with their quadratic terms, whereas for treeless areas the best
245 model included the linear term of precipitation and the quadratic term of temperature. For forest
246 and treeless states, a global model (i.e. including all the study area) presented high explanatory
247 power ($D^2=45$ and 60% for forest and treeless areas, respectively). As noted in the Methods, the
248 global model performed poorly for savanna ($D^2=12\%$). Models considering a spatial factor with
249 multiple subareas had larger explanatory power for this area (D^2 values ranging from 15.4% to
250 33.7%; Table S1). The consensus model for this state resulting from the ensemble modeling
251 presented an averaged explained deviance of 30.3% (Table 1).

252 Our results indicate that forests will decrease in area in favor of savannas by the year
253 2070 under the RCP8.5 climate change scenario (Table 2 and Fig. 1). Forest areas are predicted
254 to lose $1.5 \pm 0.9 \times 10^6$ km². This biome is expected to cover $22 \pm 4\%$ of our study area in year
255 2070, which means a 24% (range 9-39%) reduction in comparison to its current distribution.

256 Results from the 16 out of 17 CMIP5 global climate models indicated a reduction of forest area

257 (Table S3). The general agreement shown by the projections of each one of the 17 CMIP5 global
258 climate models in relation to changes in forest area indicates that our predictions are robust
259 regarding uncertainties of the global climate models (Table 2). Changes in extent of treeless
260 areas are predicted to be of small extent ($-24 \pm 178 \times 10^3 \text{ km}^2$). Results from 8 CMIP5 climate
261 models predicted a reduction, whereas 9 models show an increase in treeless areas. This limited
262 change actually means that the percentage of the tropical and subtropical Americas covered by
263 treeless areas might not vary significantly due to climate change. As it will be discussed below,
264 this result does not mean that treeless areas might remain stable, but that the extension of some
265 treeless areas might be compensated by the contraction of others.

266 For the forest-savanna system, the largest transition area is located in the southern portion
267 of the Amazonian rainforest (Figure 2). Comparatively, minor transition areas are located north
268 of the Amazonian forest and along Central America. Within the savanna-treeless system, main
269 transition areas are located in the southern border of the North American deserts and along
270 Pacific coast in South America (Fig. 3). Our predictions indicate that, within the forest-savanna
271 system, changes in the multistate equilibrium toward savanna occur mainly in the East Amazonia
272 and North Matto Grosso regions (Fig. 4). Within the savanna-treeless transition realm, changes
273 towards savanna occur in the Peruvian and Bolivian slopes of the Andes facing west, north of the
274 Atacama Desert. Despite the overall reduction of the total forest area, our models predict an
275 increase in the probability of forest in the southern Atlantic Forest region. Shifts towards treeless
276 areas are of much lesser extent and intensity (i.e. amount of change in the transition index) than
277 those towards forest or savanna. Main areas where our models predict a shift towards treeless
278 areas are Northeastern Brazil and part of the Chaco, between Paraguay and Bolivia.

279 Our models predict an important geographical shift in the current distribution of the
280 forest–savanna transition, which is less pronounced in the case of the savanna-treeless transition
281 (Fig. 5). The largest move in forest–savanna transitions (up to 600 km westward) occurs in the
282 eastern part of the Amazon, affecting the contact areas of the Amazon with three different
283 savanna systems present in the region (Llanos, Roraima and Cerrado). Lesser shifts (up to 100
284 km northward) occur in the southern limit of the Amazonia. Regarding the savanna-treeless
285 transition line, our models predict minor shifts (up to 50 km westward) in the arid and semiarid
286 areas of West South America (i.e., Atacama, Chaco, Monte Desert). Our models suggest that the
287 shift in the transition line in this area increases towards the South, being maximal in the
288 Argentinean Monte Desert. Transition areas located in the North American deserts (i.e. Mojave,
289 Sonoran, Chihuahuan) are not expected to shift (Fig. 5).

290 Changes in the extent and geographical location of the transition areas occur
291 simultaneously with an increase of the uncertainty of the system state (Fig. 6). In the forest-
292 savanna system, the reduction of forest areas is at the expense of those areas with current lowest
293 uncertainty of being forest. A large fraction (58%) of these areas, which can be considered the
294 core of the forest biome, shift towards areas with higher uncertainty levels (Fig. 6). As a result,
295 core forest areas, which nowadays occupy $3.1 \times 10^6 \text{ km}^2$, are projected to cover $1.3 \times 10^6 \text{ km}^2$
296 (range: $0.3 - 2.4 \times 10^6 \text{ km}^2$, Table S4). The different projections resulting from the 17 CMIP
297 global climate models show consistent patterns in the changes in uncertainty of the forest-
298 savanna system, as shown by the reduced standard deviation of the predictions (Fig. 6). All 17
299 CIMP5 climate models predict a reduction in the areas of low uncertainty of being forest (Table
300 S4). Forest-savanna transition areas (i.e. those where the difference in the probability of being
301 forest and savanna is <0.2) increased on average by 32%, from $2 \times 10^6 \text{ km}^2$ to $2.7 \times 10^6 \text{ km}^2$

302 (range= 2.2 – 3.6 x10⁶ km², Table S4). A similar pattern, but much less pronounced, occurs in the
303 savanna-treeless system, with a decrease in areas with high certainty of being treeless that shift
304 towards areas of higher uncertainty (Fig. 6 and Table S5). The largest increases in uncertainty of
305 the system state, projected to occur on the forest-savanna system, are located around two areas:
306 the Amazon forest, particularly in the west, and the southern portion of the Atlantic Forest,
307 because of their shifts towards savanna and forest, respectively (Fig. 7). The largest decreases in
308 uncertainty are located in those savanna areas on the West of South America (Llanos, Roraima,
309 Northern Cerrado), which are clearly expected to shift towards savanna.

310

311 DISCUSSION

312 ~~Transitions between forests, savannas and treeless are of utmost importance for understanding~~
313 ~~major environmental issues such as desertification (Maestre et al., 2009; Schlesinger et al., 1990)~~
314 ~~and the global carbon cycle (Pacala et al., 2001), and have important socio-economical and~~
315 ~~management implications at large scales (Gifford & Howden, 2001; Hudak, 1999; Van Auken,~~
316 ~~2009). Despite the importance of this topic, no previous study has evaluated how climate change~~
317 ~~will affect these transitions areas at regional to continental scales.~~ Our results indicate that
318 climate change according to the RCP8.5 scenario of the IPCC will promote the savannization of
319 the tropical and subtropical Americas, with an increase of savannas mostly at the expense of
320 forests. Such change will also increase the extent of transition areas between savannas and
321 forests, and will promote a dramatic reduction of stable forest areas. According to current
322 knowledge, the shifts predicted in the distribution and stability of transitions areas are expected
323 to bring important changes to the biota and the provision of ecosystem services such as C
324 sequestration, climate regulation and food production in one of the most important regions
325 worldwide for biodiversity and human wellbeing (MEA, 2005).

326 Our modeling approach, which relies on niche modeling theory and focuses exclusively
327 on the climatic controls of transitions, does not take into account other factors that have been
328 identified as interacting with climate drivers, such as feedbacks between tree cover and climate,
329 particularly in the rainforest (Coe et al., 2013; Malhi et al., 2008), sea surface temperature
330 (Pereira, Costa & Malhado, 2013), CO₂ fertilization (Lapola, Oyama & Nobre, 2009) and land
331 uses (Nepstad et al., 2008). In the same vein, our models use average annual values, and do not
332 consider intra- and inter-annual variability in rainfall and temperature, which have been
333 described to have significant effects in driving tree cover (Holmgren et al., 2013; Malhi et al.,
334 2008). Notwithstanding, the overall agreement (**discussed below**) between our projections and
335 those obtained by previous studies using more complex models regarding the direction, spatial
336 location and order of magnitude of the vegetation changes observed at a regional scale makes us
337 confident on the results reported here. ~~Furthermore, the relatively reduced variability of the
338 projections obtained from each one of the 17 CMIP5 global climate models used also indicates
339 that our predictions are robust regarding the uncertainty of the models using the Representative
340 Concentration Pathway 8.5 for the year 2070.~~

341

342 CLIMATE-CHANGE IMPACTS ON THE EXTENT OF SAVANNA, FOREST AND

343 TREELESS AREAS

344 Our models predict that climate change will increase the extent of savannas in the Americas by
345 12% (**range=5-19%, average increase=1.5 x10⁶ km²**) at the expense mostly of forests, which will
346 decrease by 24% (**range= 9-38%, average decrease= 1.5 x10⁶ km²**) and in much less extent of
347 treeless areas. Overall this result matches the process of savannization predicted for the area for
348 the 21st century because of climate change (Franchito, Rao & Fernandez, 2012; Hutyrá et al.,

349 2005; Cook & Vizy, 2008; Salazar & Nobre, 2010). In agreement with previous results (Cook,
350 Zeng & Yoon, 2012; Franchito, Rao & Fernandez, 2012; Hutyra et al., 2005; Salazar & Nobre,
351 2010), our projections indicate that major increases of savanna **will occur** at the expense of the
352 Amazon rainforest, particularly at its south and southeastern portions. The amount of predicted
353 reduction of forest, **ranging from 9% to 38%**, falls within the range predicted by other authors for
354 South America (Cook & Vizy, 2008; Hutyra et al., 2005; Salazar, Nobre & Oyama, 2007;
355 Zelazowski et al., 2011). Previous studies have indicated that a larger stability of the forest in the
356 Mata Atlantica in comparison with the Amazon under a climate-change scenario (Cook, Zeng &
357 Yoon, 2012). Our results go one step further and predict a strong increase of the **probability of**
358 **being forest** in this area. The forest of the Mata Atlantica is strongly fragmented, and only around
359 10% of its original area actually remains (Saatchi et al., 2001). Our findings indicate that in this
360 region management actions designed to increase tree cover could take advantage of this positive
361 inertia towards the forest.

362 In comparison with the transitions between forest and savanna, our prediction of
363 transitions between savanna and treeless areas are overall small in extent, with a decrease of <1%
364 of the treeless areas ($2.4 \times 10^4 \text{ km}^2$). The impacts of climate change on the extent of drylands have
365 been much less explored than those on forests, particularly in the Amazon region. Existing work
366 indicates an overall increase in aridity and the extent of drylands in most the arid areas of
367 tropical and subtropical Americas (Feng & Fu, 2013; Seager et al., 2007). Our results partially
368 match these patterns, since they predict a general increase in the extent of the Caatinga (NE
369 Brazil) and Chaco Seco (Argentina and Paraguay), and a patchy increase in the extent in North
370 American deserts. However, against current knowledge (Feng & Fu, 2013), our models predict a

371 savannization of the Atacama Desert and particularly, of the Sechura Desert, along the Peruvian
372 Pacific coast.

373 Changes in vegetation type from forest into savanna and treeless groups are expected to
374 have major effects on climate (Oyama & Nobre, 2003; Shukla, Nobre & Sellers, 1990).
375 Vegetation changes affect climate directly via changes in albedo and transpiration, the later
376 mediated through changes in rooting depth. Vegetation changes also affect climate indirectly
377 through changes in carbon cycling. Albedo increases along the gradient from forest, savanna to
378 treeless vegetation therefore increasing the amount of radiation reflected back to the atmosphere
379 and reducing surface temperature (Balling Jr, 1988). Rooting depth decreases from forest to
380 treeless vegetation, reducing the depth of the soil explored by roots and functionally reducing the
381 soil water-holding capacity (Jackson et al., 1996). A reduced soil-water capacity may decrease
382 the latent heat therefore reducing the cooling capacity of the ecosystem. Finally, carbon storage
383 is much larger in forest than in savannas and treeless vegetation in tropical areas (Saatchi et al.,
384 2011), so the transition from forest into savanna may results in a net carbon emission into the
385 atmosphere that will enhance climate warming.

386

387 CLIMATE CHANGE EFFECTS ON TRANSITION AREAS AND THE STABILITY OF THE 388 SYSTEM

389 Using the framework of alternative stable states provided by Hirota *et al.* (2011), we were able to
390 project how the transition areas between biomes and **the stability of the system** are expected to
391 change under climate change. These two related aspects have been much less explored than the
392 changes in the extent of the biomes themselves. As with the projected changes in the extent of

393 biomes, shifts in the transitions between forests and savannas were much more pronounced than
394 those between savannas and treeless areas.

395 Our models predict that climate change will promote a shift towards more unstable states,
396 yielding **more uncertainty in system state**. Two aspects of this result deserve particular attention.
397 On the one hand, the extent of the transition areas will increase by 32% on average (range=10-
398 80%), and forest-savanna transition areas, now restricted to a thin belt between both biomes
399 might become the dominant biome in large areas, particularly in the South and Eastern part of
400 Brazil. On the contrary, large stable forest areas are predicted to decrease by 58% on average
401 (range=23-90%). The climate control of vegetation types is strongest in the core (**i.e. ecological**
402 **optimum**) of their distribution and weakens towards the edges (Sala, Lauenroth & Golluscio,
403 1997). It is in the edges of the distribution of vegetation types where other factors such as
404 grazing intensity, fire, and logging become more important. The increase in uncertainty of large
405 areas of the Amazon rainforest means that these areas will likely be less resilient to
406 perturbations, and thus that they might be more sensitive to human management (Hirota et al.,
407 2011). In these areas of high uncertainty, positive feedbacks might make that small changes in
408 tree cover might induce a self-propagating shift to the alternative state (i.e. from forest to
409 savanna or from savanna to forest). In this way, fragmented landscapes with a patchy distribution
410 of forest and savanna might be more likely to turn into solely savanna landscapes, due to, for
411 example, an increase in fire frequency and extent (Malhi et al., 2008). Interestingly, and as
412 pointed out for the Mata Atlantica above, these feedbacks can also work in the opposite direction
413 and, in areas of high uncertainty, tree cover increases due to habitat management are more likely
414 to trigger the conversion of savanna to forest. Land-use changes are at present the main driver of
415 the transition between states in the study area, particularly the conversion of forest to savanna

416 and treeless areas due to deforestation (Malhi et al., 2008). Overall, our results indicate that
417 climate change will increase the importance of land use in shaping the extent of biomes during
418 the next century.

419

420 PREDICTED IMPACTS OF CLIMATE CHANGE ON BIODIVERSITY AND ECOSYSTEM
421 SERVICES

422 The Amazon rainforest is a major component of the Earth's system, regulating Earth's climate
423 (Malhi et al., 2008), and hosts up to a quarter of the world's terrestrial species (Barthlott &
424 Winiger, 1998). Rapid transition from one vegetation type to another will certainly result in
425 major biodiversity losses (Sala et al., 2005). Our models predict a shift of the forest-savanna
426 transition area of up to 600 km in the eastern Amazon for year 2070. Given the magnitude and
427 speed of this change, a pertinent question here is to what extent species will be able to keep pace
428 with climatic changes to reach the equilibrium (Loarie et al., 2009). Although our understanding
429 of colonization processes under climate change is still limited, current models indicate that
430 species will lag behind projected climate shifts (Nathan et al., 2011; Prasad et al., 2013). The
431 mismatch between climatic change velocity and colonization rates is expected to be exacerbated
432 in flat reliefs (Loarie et al., 2009), which are dominant in the Amazonian Basin. In this area, our
433 models predict the largest shifts from forest to savanna suggesting a high risk for species
434 extinctions. However, as it has been described for tree species colonization after the ice caps
435 retreated during the Holocene, isolated habitat patches outside the core distribution range of the
436 biome could play key role in tracking climate change (Anderson et al., 2006; McLachlan, Clark
437 & Manos, 2005; Parducci et al., 2012). In our case, for example, small savanna patches currently

438 embedded in a forest matrix, could serve as colonizing source for the surrounding landscape
439 when climate potentially in the area change from forest to savanna.

440 The portfolio of ecosystem services provided by forest, savannas and treeless vegetation
441 types are drastically different. For example, savanna and grasslands in tropical and subtropical
442 America constitute one of the main providers of food, particularly protein, of the world (FAO,
443 2007). As the reverse side of the ecosystem services linked to rainforest, predicted changes might
444 have a positive impact on the provisioning of food (MEA, 2005). We predicted an increase in the
445 extent of transition areas and in the uncertainty of the system. This means that alternative states
446 (i.e. forest, savanna, treeless) are likely to be more evenly distributed at a small scale (i.e. a finer
447 grain distribution) and that localities are expected to tip from one state to another more easily. As
448 a result, ecosystem services provided at a local scale are likely to be more diversified but also
449 more unpredictable, since larger portions of our study area might contain a combination of
450 different biomes that will change more frequently. Food, timber, climate amelioration, clean
451 water, recreation and conservation are ecosystem services that will be affected by vegetation
452 transitions. These changes in the portfolio of ecosystem services resulting from vegetation
453 transitions will affect different groups of stakeholders because they value ecosystem services
454 differently.

455

456 **Acknowledgements**

457 We acknowledge support for this effort from US National Science Foundation DEB-1242747,
458 1235828, National Academies Keck Frontiers Initiative award 025512, and SARAS (South
459 American Institute for Resilience and Sustainability Studies) Institute. FTM is supported by the
460 European Research Council under the European Community's Seventh Framework Programme

461 (FP7/2007-2013)/ERC Grant agreement 242658 (BIOCOM). We acknowledge the World
462 Climate Research Programme's Working Group on Coupled Modelling, which is responsible for
463 CMIP, and the climate modeling groups (listed in Table S2 of this paper) for producing and
464 making available their model output. For CMIP the U.S. Department of Energy's Program for
465 Climate Model Diagnosis and Intercomparison provides coordinating support and led
466 development of software infrastructure in partnership with the Global Organization for Earth
467 System Science Portals.

468
469 **REFERENCES**

- 470 Anadón, J. D., Sala, O. E., Turner, B. L. & Bennett, E. M. (2014) Effect of woody plant encroachment on
471 livestock production: A comparison of North and South America. *Proceedings of National*
472 *Academy of Sciences*, **in press**.
- 473 Anderson, L. L., Hu, F. S., Nelson, D. M., Petit, R. J. & Paige, K. N. (2006) Ice-age endurance: DNA
474 evidence of a white spruce refugium in Alaska. *Proceedings of the National Academy of Sciences*,
475 **103**, 12447-12450.
- 476 Araújo, M. B. & New, M. (2007) Ensemble forecasting of species distributions. *Trends in Ecology &*
477 *Evolution*, **22**, 42-47.
- 478 Araújo, M. B. & Peterson, A. T. (2012) Uses and misuses of bioclimatic envelope modeling. *Ecology*, **93**,
479 1527-1539.
- 480 Bailey, R. G. & Ropes, L. (1998) *Ecoregions: the ecosystem geography of the oceans and continents*.
481 Springer New York.
- 482 Balling Jr, R. C. (1988) The climatic impact of a Sonoran vegetation discontinuity. *Climatic Change*, **13**,
483 99-109.
- 484 Barthlott, W. & Winiger, M. (1998) *Biodiversity: a challenge for development research and policy*.
485 Springer.
- 486 Bartholome, E. & Belward, A. S. (2005) GLC2000: a new approach to global land cover mapping from
487 Earth observation data. *International Journal of Remote Sensing*, **26**, 1959-1977.
- 488 Burnham, K. P. & Anderson, D. R. (2002) *Model selection and multimodel inference: a practical*
489 *information-theoretic approach*. Springer.
- 490 Coe, M. T., Marthews, T. R., Costa, M. H., Galbraith, D. R., Greenglass, N. L., Imbuzeiro, H. M., Levine,
491 N. M., Malhi, Y., Moorcroft, P. R. & Muza, M. N. (2013) Deforestation and climate feedbacks
492 threaten the ecological integrity of south-southeastern Amazonia. *Philosophical Transactions of*
493 *the Royal Society B: Biological Sciences*, **368**.
- 494 Cook, B., Zeng, N. & Yoon, J.-H. (2012) Will Amazonia Dry Out? Magnitude and Causes of Change from
495 IPCC Climate Model Projections. *Earth Interactions*, **16**.
- 496 Cook, K. H. & Vizy, E. K. (2008) Effects of Twenty-First-Century Climate Change on the Amazon Rain
497 Forest. *Journal of Climate*, **21**.

- 498 Eldridge, D. J., Bowker, M. A., Maestre, F. T., Roger, E., Reynolds, J. F. & Whitford, W. G. (2011)
 499 Impacts of shrub encroachment on ecosystem structure and functioning: towards a global
 500 synthesis. *Ecology Letters*, **14**, 709-722.
- 501 FAO (2007) *Gridded livestock of the world 2007*, by G.R.W. Wint and T.P. Robinson. Food and Agriculture
 502 Organization of the United Nations, Rome.
- 503 Feng, S. & Fu, Q. (2013) Expansion of global drylands under a warming climate. *Atmospheric Chemistry &*
 504 *Physics*, **13**.
- 505 Franchito, S. H., Rao, V. B. & Fernandez, J. P. R. (2012) Tropical land savannization: impact of global
 506 warming. *Theoretical and applied climatology*, **109**, 73-79.
- 507 Gang, C. C., Zhou, W., Li, J. L., Chen, Y. Z., Mu, S. J., Ren, J. Z., Chen, J. M. & Groisman, P. Y. (2013)
 508 Assessing the Spatiotemporal Variation in Distribution, Extent and NPP of Terrestrial Ecosystems
 509 in Response to Climate Change from 1911 to 2000. *Plos One*, **8**.
- 510 Gedney, N. & Valdes, P. J. (2000) The effect of Amazonian deforestation on the northern hemisphere
 511 circulation and climate. *Geophysical Research Letters*, **27**, 3053-3056.
- 512 Gehrig-Fasel, J., Guisan, A. & Zimmermann, N. E. (2007) Tree line shifts in the Swiss Alps: Climate
 513 change or land abandonment? *Journal of vegetation science*, **18**, 571-582.
- 514 Gifford, R. M. & Howden, M. (2001) Vegetation thickening in an ecological perspective: significance to
 515 national greenhouse gas inventories. *Environmental Science & Policy*, **4**, 59-72.
- 516 Hansen, M. C., DeFries, R. S., Townshend, J. R. G., Carroll, M., Dimiceli, C. & Sohlberg, R. A. (2003)
 517 Global percent tree cover at a spatial resolution of 500 meters: First results of the MODIS
 518 vegetation continuous fields algorithm. *Earth Interactions*, **7**, 1-15.
- 519 Hartley, S., Harris, R. & Lester, P. J. (2006) Quantifying uncertainty in the potential distribution of an
 520 invasive species: climate and the Argentine ant. *Ecology Letters*, **9**, 1068-1079.
- 521 Havstad, K. M., Peters, D. P. C., Skaggs, R., Brown, J., Bestelmeyer, B. T., Fedrickson, E., Herrick, J. E. &
 522 Wright, J. (2007) Ecological services to and from rangelands of the United States. *Ecological*
 523 *Economics*, **64**, 261-268.
- 524 Hirota, M., Holmgren, M., Van Nes, E. H. & Scheffer, M. (2011) Global Resilience of Tropical Forest and
 525 Savanna to Critical Transitions. *Science*, **334**, 232-235.
- 526 Holmgren, M., Hirota, M., van Nes, E. H. & Scheffer, M. (2013) Effects of interannual climate variability
 527 on tropical tree cover. *Nature Climate Change*.
- 528 Hudak, A. T. (1999) Rangeland mismanagement in South Africa: failure to apply ecological knowledge.
 529 *Human Ecology*, **27**, 55-78.
- 530 Hutyrá, L., Munger, J., Nobre, C., Saleska, S., Vieira, S. u. & Wofsy, S. (2005) Climatic variability and
 531 vegetation vulnerability in Amazonia. *Geophysical Research Letters*, **32**.
- 532 IPCC (2013) *Climate Change 2013: The Physical Science Basis. Contribution of Working Group I to the*
 533 *Fifth Assessment Report of the Intergovernmental Panel on Climate Change* Cambridge
 534 University Press, Cambridge, United Kingdom and New York, NY, USA.
- 535 Jackson, R., Canadell, J., Ehleringer, J., Mooney, H., Sala, O. & Schulze, E. (1996) A global analysis of
 536 root distributions for terrestrial biomes. *Oecologia*, **108**, 389-411.
- 537 Kark, S. & Van Rensburg, B. J. (2006) Ecotones: marginal or central areas of transition? *Israel Journal of*
 538 *Ecology & Evolution*, **52**, 29-53.
- 539 Kulmatiski, A. & Beard, K. H. (2013) Woody plant encroachment facilitated by increased precipitation
 540 intensity. *Nature Climate Change*, **3**, 833-837.
- 541 Lapola, D. M., Oyama, M. D. & Nobre, C. A. (2009) Exploring the range of climate biome projections for
 542 tropical South America: The role of CO₂ fertilization and seasonality. *Global Biogeochemical*
 543 *Cycles*, **23**.
- 544 Loarie, S. R., Duffy, P. B., Hamilton, H., Asner, G. P., Field, C. B. & Ackerly, D. D. (2009) The velocity of
 545 climate change. *Nature*, **462**, 1052-1055.

- 546 Maestre, F. T., Bowker, M. A., Puche, M. D., Belén Hinojosa, M., Martínez, I., García-Palacios, P.,
 547 Castillo, A. P., Soliveres, S., Luzuriaga, A. L. & Sánchez, A. M. (2009) Shrub encroachment can
 548 reverse desertification in semi-arid Mediterranean grasslands. *Ecology Letters*, **12**, 930-941.
- 549 Malhi, Y., Roberts, J. T., Betts, R. A., Killeen, T. J., Li, W. & Nobre, C. A. (2008) Climate change,
 550 deforestation, and the fate of the Amazon. *Science*, **319**, 169-172.
- 551 Marmion, M., Parviainen, M., Luoto, M., Heikkinen, R. K. & Thuiller, W. (2009) Evaluation of consensus
 552 methods in predictive species distribution modelling. *Diversity and Distributions*, **15**, 59-69.
- 553 McLachlan, J. S., Clark, J. S. & Manos, P. S. (2005) Molecular indicators of tree migration capacity under
 554 rapid climate change. *Ecology*, **86**, 2088-2098.
- 555 MEA (2003) *Ecosystems and human well-being: A framework for assessment*. Island Press, Washington,
 556 DC.
- 557 MEA (2005) *Ecosystems and Human Well-being: Synthesis*. Island Press, Washington, DC.
- 558 Meehl, G. A., Arblaster, J. M. & Tebaldi, C. (2005) Understanding future patterns of increased
 559 precipitation intensity in climate model simulations. *Geophysical Research Letters*, **32**.
- 560 Myers, N., Mittermeier, R. A., Mittermeier, C. G., Da Fonseca, G. A. & Kent, J. (2000) Biodiversity
 561 hotspots for conservation priorities. *Nature*, **403**, 853-858.
- 562 Nathan, R., Horvitz, N., He, Y., Kuparinen, A., Schurr, F. M. & Katul, G. G. (2011) Spread of North
 563 American wind-dispersed trees in future environments. *Ecology Letters*, **14**, 211-219.
- 564 Nepstad, D. C., Stickler, C. M., Soares-Filho, B. & Merry, F. (2008) Interactions among Amazon land use,
 565 forests and climate: prospects for a near-term forest tipping point. *Philosophical Transactions of
 566 the Royal Society B: Biological Sciences*, **363**, 1737-1746.
- 567 Oyama, M. D. & Nobre, C. A. (2003) A new climate-vegetation equilibrium state for tropical South
 568 America. *Geophysical Research Letters*, **30**.
- 569 Pacala, S. W., Hurtt, G. C., Baker, D., Peylin, P., Houghton, R. A., Birdsey, R. A., Heath, L., Sundquist, E.
 570 T., Stallard, R. & Ciais, P. (2001) Consistent land-and atmosphere-based US carbon sink
 571 estimates. *Science*, **292**, 2316-2320.
- 572 Parducci, L., Jørgensen, T., Tollefsrud, M. M., Elverland, E., Alm, T., Fontana, S. L., Bennett, K. D.,
 573 Haile, J., Matetovici, I. & Suyama, Y. (2012) Glacial survival of boreal trees in northern
 574 Scandinavia. *Science*, **335**, 1083-1086.
- 575 Parmesan, C. (2006) Ecological and evolutionary responses to recent climate change. *Annu. Rev. Ecol.
 576 Evol. Syst.*, **37**, 637-669.
- 577 Parmesan, C. & Yohe, G. (2003) A globally coherent fingerprint of climate change impacts across natural
 578 systems. *Nature*, **421**, 37-42.
- 579 Paruelo, J. M., Lauenroth, W. K., Epstein, H. E., Burke, I. C., Aguiar, M. R. & Sala, O. E. (1995) Regional
 580 climatic similarities in the temperate zones of North and South America. *Journal of
 581 Biogeography*, **22**, 915-925.
- 582 Peñuelas, J., Sardans, J., Estiarte, M., Ogaya, R., Carnicer, J., Coll, M., Barbeta, A., Rivas-Ubach, A.,
 583 Llusà, J. & Garbulsy, M. (2013) Evidence of current impact of climate change on life: a walk
 584 from genes to the biosphere. *Global Change Biology*, **19**, 2303-2338.
- 585 Pereira, M. P. S., Costa, M. H. & Malhado, A. C. M. (2013) Vegetation patterns in South America
 586 associated with rising CO₂: uncertainties related to sea surface temperatures. *Theoretical and
 587 applied climatology*, **111**, 569-576.
- 588 Prasad, A. M., Gardiner, J. D., Iverson, L. R., Matthews, S. N. & Peters, M. (2013) Exploring tree species
 589 colonization potentials using a spatially explicit simulation model: implications for four oaks
 590 under climate change. *Global Change Biology*, **19**, 2196-2208.
- 591 Saatchi, S., Agosti, D., Alger, K., Delabie, J. & Musinsky, J. (2001) Examining fragmentation and loss of
 592 primary forest in the southern Bahian Atlantic forest of Brazil with radar imagery. *Conservation
 593 Biology*, **15**, 867-875.

- 594 Saatchi, S. S., Harris, N. L., Brown, S., Lefsky, M., Mitchard, E. T., Salas, W., Zutta, B. R., Buermann,
 595 W., Lewis, S. L., Hagen, S., Petrova, S., White, L., Silman, M. & Morel, A. (2011) Benchmark
 596 map of forest carbon stocks in tropical regions across three continents. *Proc Natl Acad Sci U S A*,
 597 **108**, 9899-904.
- 598 Sala, O. E., Lauenroth, W. K. & Golluscio, R. A. (1997) Plant functional types in temperate semi-arid
 599 regions. *Plant functional types* (eds T. M. Smith, H. H. Shugart & F. I. Woodward). Cambridge
 600 University Press, Cambridge.
- 601 Sala, O. E., van Vuuren, D., Pereira, H., Lodge, D., J, A., S, C. G., A, D., V, W. & M, X. (2005)
 602 Biodiversity across scenarios. *Ecosystems and Human Well-Being: Scenarios: Scenarios* (eds C. S.
 603 R, P. P. L, B. E. M & Z. M), pp. 375-408. Island press, Washington DC.
- 604 Salazar, L. F. & Nobre, C. A. (2010) Climate change and thresholds of biome shifts in Amazonia.
 605 *Geophysical Research Letters*, **37**.
- 606 Salazar, L. F., Nobre, C. A. & Oyama, M. D. (2007) Climate change consequences on the biome
 607 distribution in tropical South America. *Geophysical Research Letters*, **34**.
- 608 Sankaran, M., Hanan, N. P., Scholes, R. J., Ratnam, J., Augustine, D. J., Cade, B. S., Gignoux, J.,
 609 Higgins, S. I., Le Roux, X. & Ludwig, F. (2005) Determinants of woody cover in African savannas.
 610 *Nature*, **438**, 846-849.
- 611 Schlesinger, W. H., Reynolds, J. F., Cunningham, G. L., Huenneke, L. F., Jarrell, W. M., Virginia, R. A. &
 612 Whitford, W. G. (1990) Biological feedbacks in global desertification. *Science(Washington)*, **247**,
 613 1043-1048.
- 614 Seager, R., Ting, M., Held, I., Kushnir, Y., Lu, J., Vecchi, G., Huang, H.-P., Harnik, N., Leetmaa, A. &
 615 Lau, N.-C. (2007) Model projections of an imminent transition to a more arid climate in
 616 southwestern North America. *Science*, **316**, 1181-1184.
- 617 Shukla, J., Nobre, C. & Sellers, P. (1990) Amazon deforestation and climate change.
 618 *Science(Washington)*, **247**, 1322-1325.
- 619 Smith, T. B., Kark, S., Schneider, C. J., Wayne, R. K. & Moritz, C. (2001) Biodiversity hotspots and
 620 beyond: the need for preserving environmental transitions. *Trends in Ecology & Evolution*, **16**,
 621 431.
- 622 Smith, T. B., Wayne, R. K., Girman, D. J. & Bruford, M. W. (1997) A role for ecotones in generating
 623 rainforest biodiversity. *Science*, **276**, 1855-1857.
- 624 Staver, A. C., Archibald, S. & Levin, S. A. (2011) The global extent and determinants of savanna and
 625 forest as alternative biome states. *Science*, **334**, 230-232.
- 626 Sturm, M., Racine, C. & Tape, K. (2001) Climate change: Increasing shrub abundance in the Arctic.
 627 *Nature*, **411**, 546-547.
- 628 Taylor, K. E., Stouffer, R. J. & Meehl, G. A. (2012) An Overview of CMIP5 and the Experiment Design.
 629 *Bulletin of the American Meteorological Society*, **93**.
- 630 Van Auken, O. (2009) Causes and consequences of woody plant encroachment into western North
 631 American grasslands. *Journal of Environmental Management*, **90**, 2931-2942.
- 632 Walther, G.-R. (2010) Community and ecosystem responses to recent climate change. *Philosophical
 633 Transactions of the Royal Society B: Biological Sciences*, **365**, 2019-2024.
- 634 Williams, R., Duff, G., Bowman, D. & Cook, G. (1996) Variation in the composition and structure of
 635 tropical savannas as a function of rainfall and soil texture along a large-scale climatic gradient in
 636 the Northern Territory, Australia. *Journal of Biogeography*, **23**, 747-756.
- 637 Zelazowski, P., Malhi, Y., Huntingford, C., Sitch, S. & Fisher, J. B. (2011) Changes in the potential
 638 distribution of humid tropical forests on a warmer planet. *Philos Trans A Math Phys Eng Sci*, **369**,
 639 137-60.

Grassland-woodland transitions Special Feature

641

642

643 **Figure Legends**

644

645 **Fig 1.** Spatial projection of the three alternative states (forest, savanna and treeless areas) for the
646 present time (1950-2000) and for the year 2070 under the RCP8.5 scenario in the tropical and
647 subtropical Americas.

648

649 **Fig 2.** Transition map for the forest-savanna system for the present time (1950-2000) and for the
650 year 2070 under the RCP8.5 scenario in the tropical and subtropical Americas. For the year
651 2070, the mean value of the 17 transition maps resulting from the 17 CMIP5 global climate
652 models is shown. A histogram with the total amount of area of each class can be found in Fig. 6
653 (Top). The total area of each class for each one of the 17 transition maps resulting from the 17
654 CMIP5 global climate models can be found in Table S4.

655

656 **Fig 3.** Transition map for savanna-treeless system for the present time (1950-2000) and for the
657 year 2070 under the RCP8.5 scenario in the tropical and subtropical Americas. For the year
658 2070, the mean value of the 17 transition maps resulting from the 17 CMIP5 global climate
659 models is shown. A histogram with the total amount of area of each class can be found in Fig. 6
660 (Bottom). Rest of legend as in Fig. 2.

661

662 **Fig 4.** Projected shift towards forest, savanna or treeless states for the year 2070 under the
663 RCP8.5 scenario in the tropical and subtropical Americas. Shifts are estimated as the difference
664 between the transition index in the present time and the year 2070 for the forest-savanna and the
665 savanna-treeless systems. The mean value of the projected shifts for the 17 transition maps
666 resulting from the 17 CMIP5 global climate models is shown. Beige area indicates those cells

667 where the change in the probability transition is below 0.1. Darker tones of green, red and blue
668 indicate stronger shifts toward forest, savanna and treeless areas respectively.

669

670 **Fig 5.** Transition areas for the forest-savanna (left) and the savanna-treeless systems (right) in the
671 present time and the year 2070 under the RCP8.5 scenario. For a given transition (i.e. forest-
672 savanna), transition areas are defined as those cells in which the difference between the two
673 alternative systems is less than 0.2. The mean value of the 17 transition maps for the year 2070
674 resulting from the 17 CMIP5 global climate models was used as base transition map.

675

676 **Fig 6.** Projected area under different classes of the transition index for the present (1950-2000)
677 and under the RCP8.5 scenario for the year 2070 for the forest-savanna (Top) and the savanna-
678 treeless transitions (Bottom). Forest-savanna transition index is calculated as $p(\text{forest}) -$
679 $p(\text{savanna})$. Savanna transition index is calculated as $p(\text{savanna}) - p(\text{treeles})$. Values closer to 1
680 and -1 indicates lower uncertainty whereas values closer to 0 indicates higher uncertainty. Mean
681 values and standard deviation of the 17 CMIP5 global climate models are shown. Results for
682 each CMIP5 global climate model are shown in Figs. S4 and S5. Area in 10^3 km^2 . Note that the
683 total area of savanna is the sum of the savanna areas in both transition systems. The spatial
684 representation of this histogram can be found in Figs. 2 and 3.

685

686 **Fig 7.** Changes in the uncertainty of the forest-savanna transition between the present (1950-
687 2000) and the RCP8.5 scenario (2070) in the tropical and subtropical Americas. The change in
688 uncertainty is calculated as the change in the transition index between the two projections (i.e.
689 1950-2000 and 2070). The mean value resulting from analysis of the 17 CMIP5 global climate

Grassland-woodland transitions Special Feature

690 models is shown. Positive values of uncertainty indicate areas where the probability of tipping
691 between forest and savanna will increase due to climate change.

692

693 **Table 1.** Candidate climatic models fitted to the distribution of forest, savanna and treeless areas
 694 in the tropical and subtropical Americas. For each model, the explained deviance (D^2) and
 695 Akaike Information Criterion (AIC) value are shown. For each state, the selected model is in
 696 bold. For the Savanna, the best global model (i.e, that with $D^2 = 12.29\%$) was not used and the
 697 value in brackets represents the explained deviance of the model finally employed. In this case,
 698 the D^2 value represents weighted mean of the D^2 values of the 20% best multi-zone models (see
 699 Methods and Table S1 in Supporting Information). P=Mean annual precipitation; T=Mean
 700 annual temperature, ARIDITY=Aridity index (P/Potential evapotranspiration)

701

702

Model	Forest		Savanna		Treeless	
	D^2	AIC	D^2	AIC	D^2	AIC
P	39.30	2230.60	1.69	4029.92	65.02	946.43
P ²	44.52	2041.20	10.35	3677.38	56.97	1165.07
T	24.79	2762.85	0.01	4098.74	28.05	1942.20
T ²	24.81	2764.23	4.29	3925.37	29.37	1908.62
P ² +T	45.64	2002.16	10.35	3679.19	56.79	1172.06
T ² +P	41.76	2144.44	5.35	3884.16	66.84	901.23
P ² +T ²	45.88	1995.36	12.29 (30.34)	3601.67	56.97	1169.33
ARIDITY	32.38	2484.60	0.99	4058.49	58.97	1109.37
ARIDITY ²	38.65	2256.38	4.02	3936.52	59.50	1096.95
P/T	15.30	3111.09	0.32	4086.00	27.80	1948.89
(P/T) ²	33.02	2462.86	0.43	4083.42	-	-

703

704

705 **Table 2.** Projected representation of forest, savanna and treeless areas in our study area for the
 706 present time (1950-2000) and for 2070 under the RCP8.5 scenario. For the 1950-2000 period,
 707 real values (i.e. observed from the data, not modeled) are shown in brackets. Mean values and
 708 standard deviation from the 17 downscaled and calibrated CMIP5 global climate models are
 709 indicated. Results for each CMIP5 global climate model are shown in Fig. S3

710

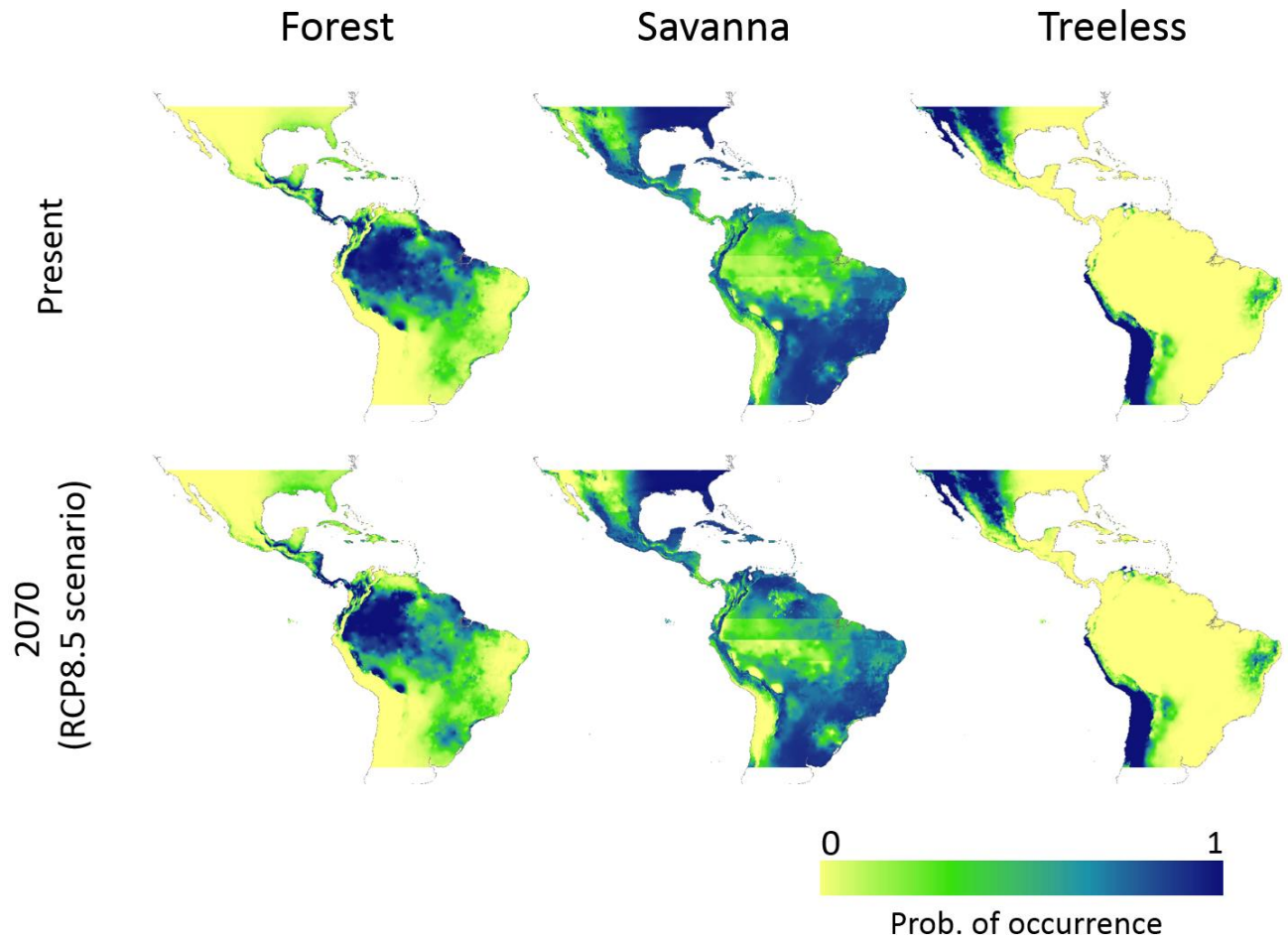
711

	1950-2000		2070 RCP8.5		Change	
	Area ($\times 10^3$ km ²)	%	Area ($\times 10^3$ km ²)	%	Area ($\times 10^3$ km ²)	Change (%)
Forest	6235	29 (31)	4760 \pm 896	22 \pm 4	-1474 \pm 896	-24 (-38 - -9)
Savanna	12765	58 (52)	14263 \pm 921	65 \pm 4	1498 \pm 921	12 (5 - 19)
Treeless	2847	13 (17)	2823 \pm 178	13 \pm 1	-24 \pm 178	-1 (-7 - 5)

712

713 **Fig 1.**

714



715

716

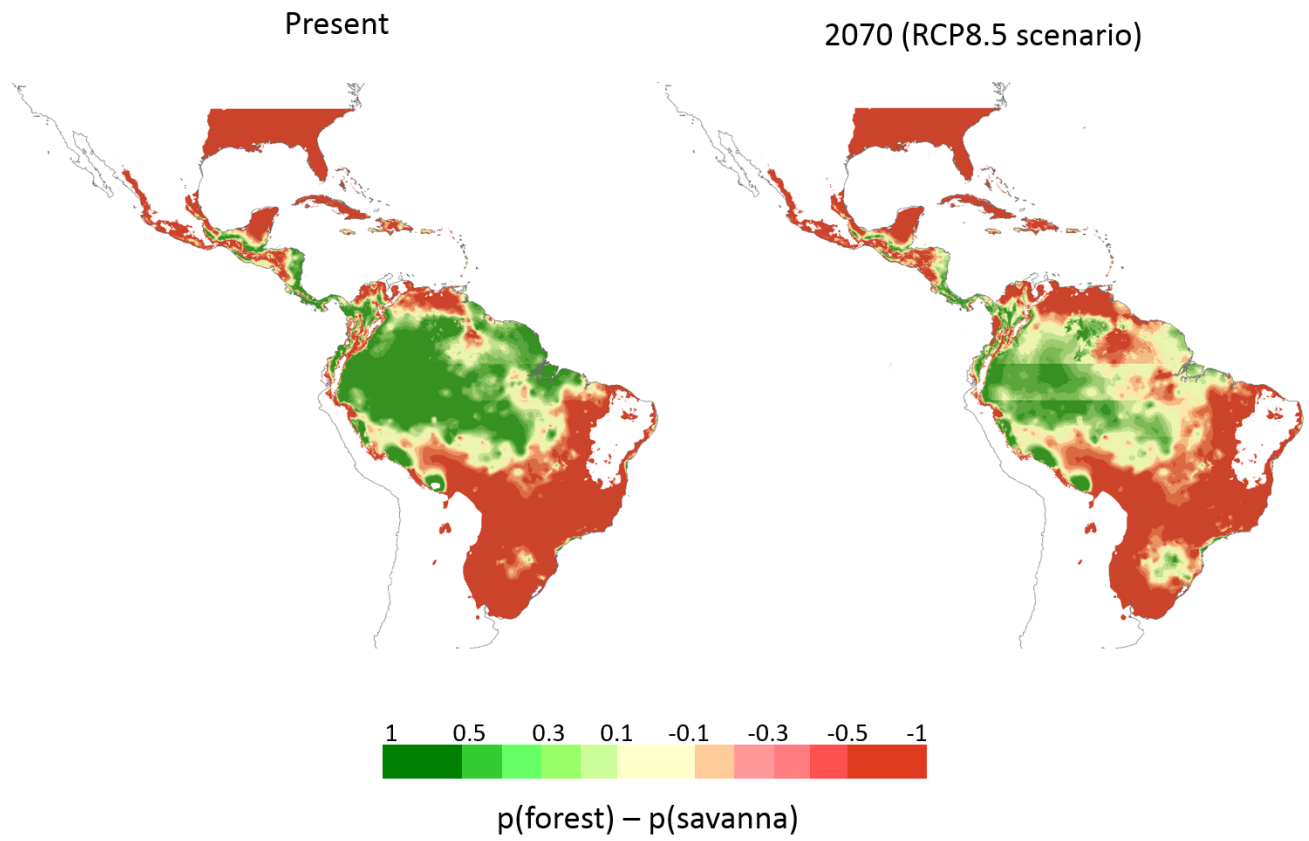
717

718 **Fig 2**

719

720

Forest-savanna transition



721

722

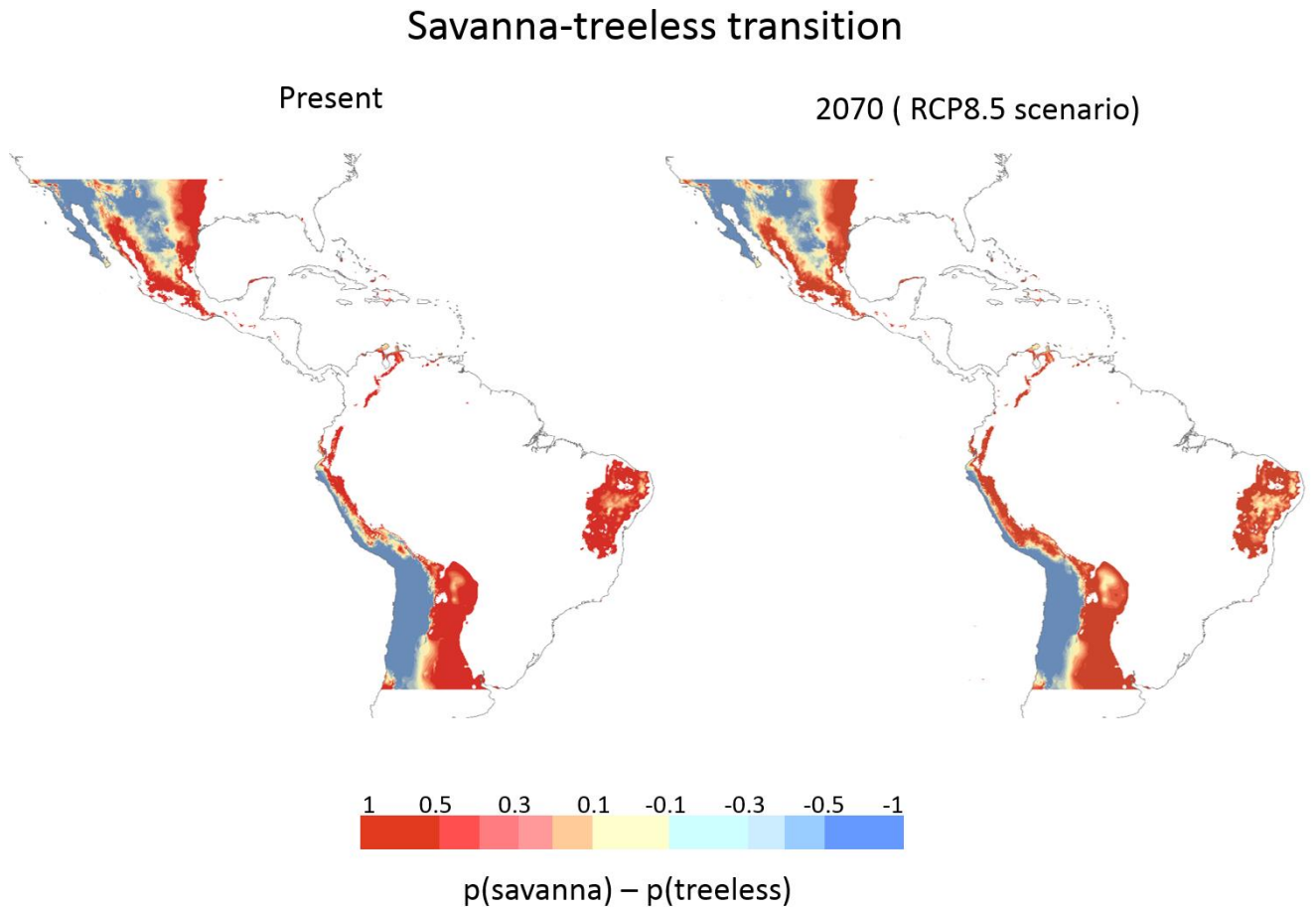
723

724

725 **Fig 3.**

726

727



728

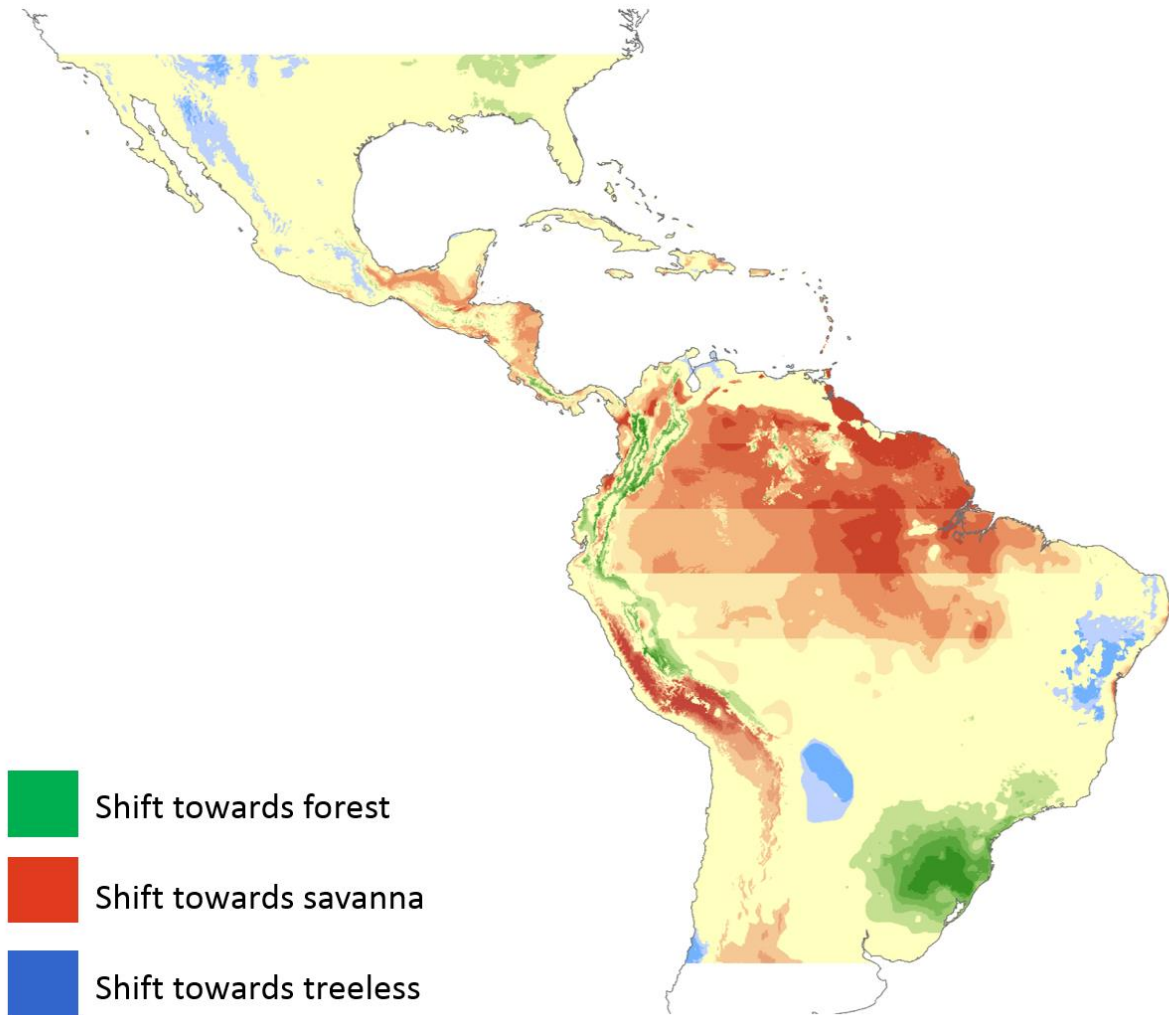
729

730

731

732 **Fig 4.**

733

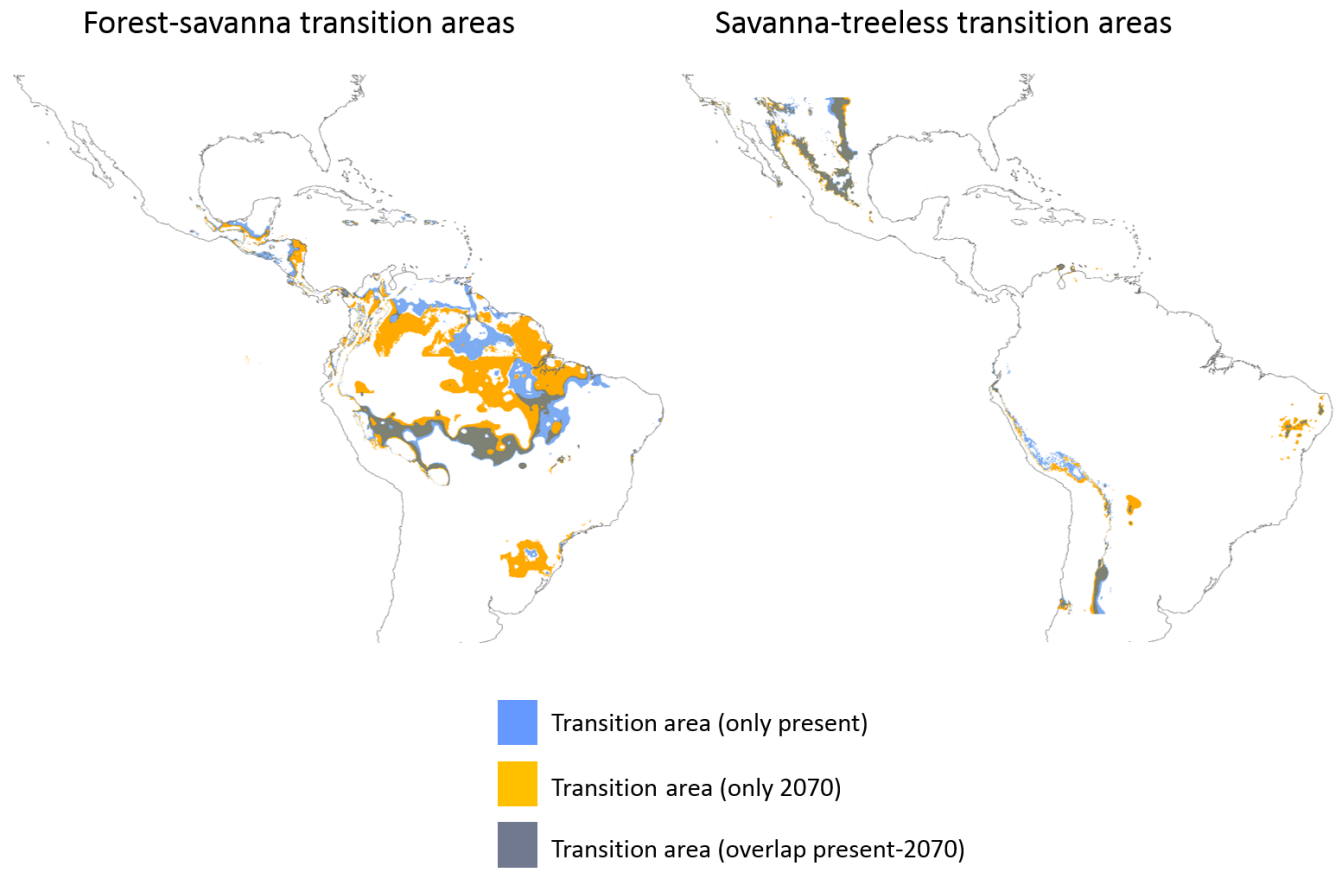


734

735

736 **Fig 5.**

737



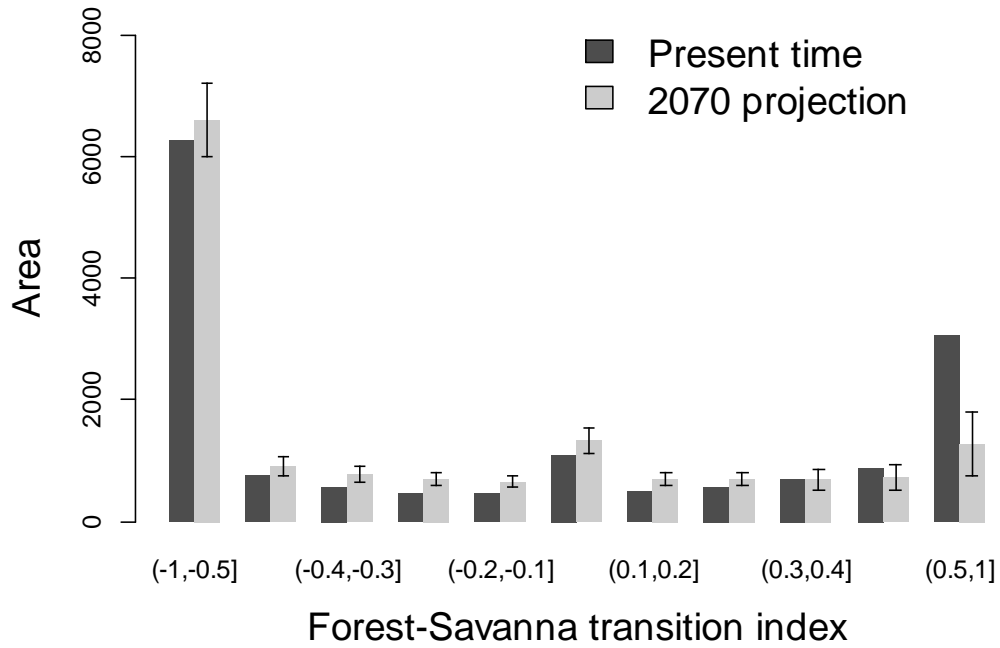
738

739

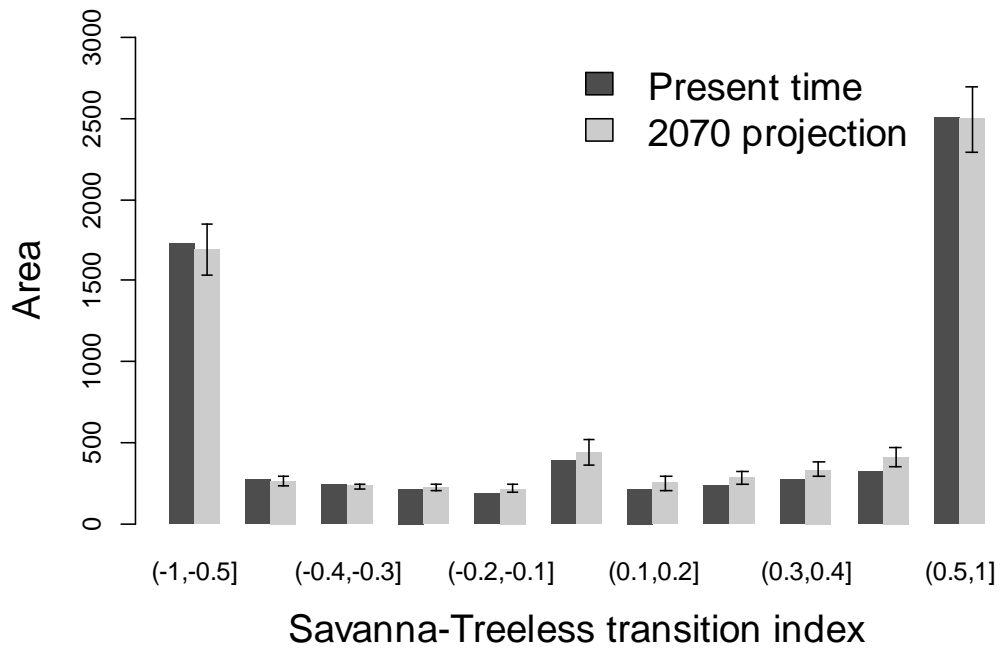
740

741

742 **Fig 6.**



743



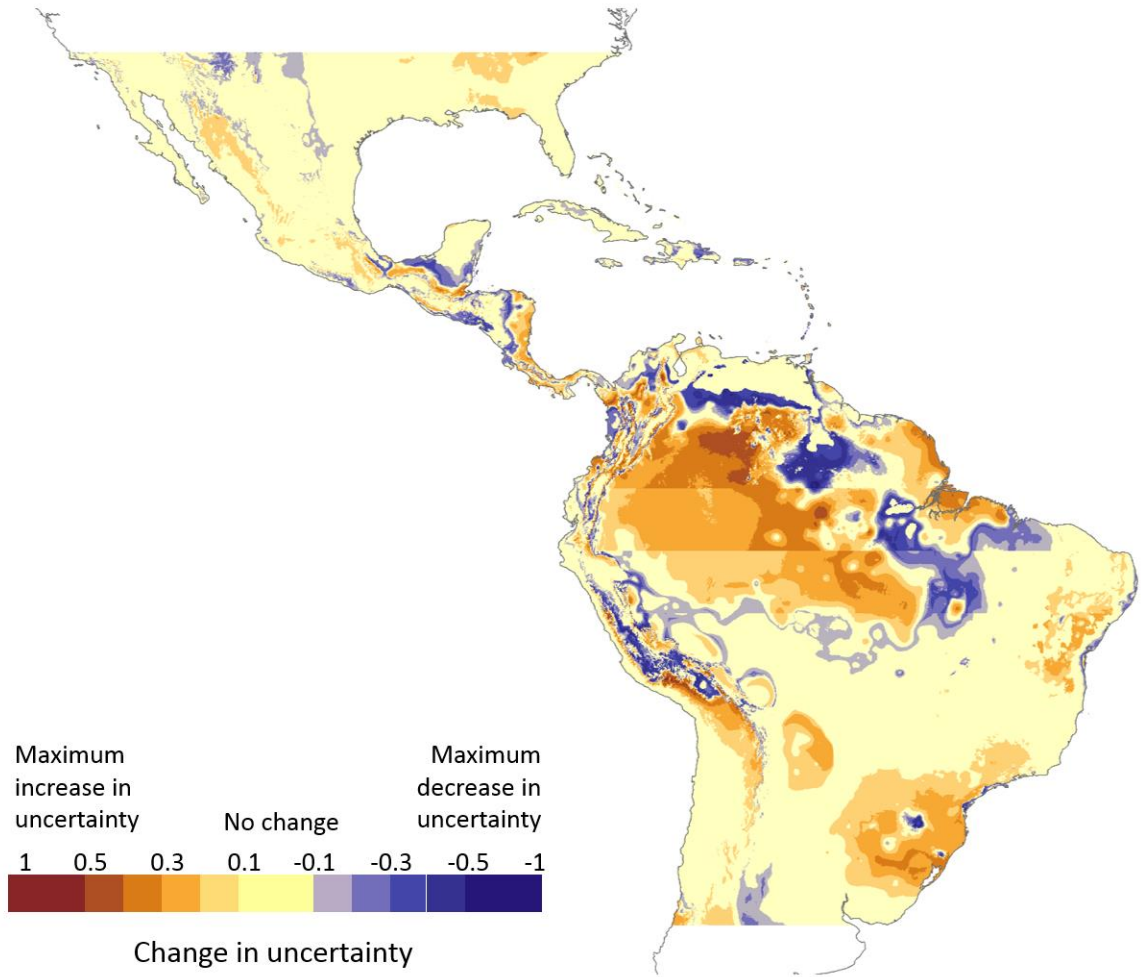
744

745

746

747 **Fig 7.**

748



749

750

751

752

753 **SUPPORTING INFORMATION**

754

755 **Table S1.** 20% best models fitted to the distribution of savanna. In all cases, the models include
 756 the same climatic variables (i.e. best global model P^2+T^2 , see Table 1) plus a spatial factor. All
 757 best models included the spatial factor describing three subareas, defined by the latitudinal limits
 758 Lim1 and Lim2. Latitudinal limits for the entire study area are 35°N and -35N. The minimum
 759 latitudinal width of a subarea was 5°. For example, the model ranked first included a spatial
 760 factor with three subareas with limits: 35°N - 20°N, 20°N - -5°N and 5°N - -35°N

Rank	N subareas	Lim1	Lim2	D2	AIC
1	3	20°	-5°	33.55	2751.08
2	3	10°	-5°	33.28	2762.37
3	3	25°	-5°	31.63	2830.00
4	3	15°	-5°	32.81	2781.58
5	3	20°	0°	31.15	2849.34
6	3	10°	0°	30.26	2885.90
7	3	15°	0°	30.11	2891.87
8	3	25	0°	29.56	2914.77
9	3	5°	-5°	32.40	2798.09
10	3	20°	-10°	30.58	2872.94
11	3	30°	-5°	27.97	2979.52
12	3	25°	-10°	28.83	2944.51
13	3	20°	-15°	29.19	2929.69
14	3	5°	0°	28.99	2937.92
15	3	30°	0°	26.50	3040.08
16	3	15°	-10°	29.65	2910.80
17	3	10°	-10°	29.89	2901.21
18	3	25°	-15°	27.63	2993.68

761

762

763 **Table S2.** List of the 17 Coupled Model Intercomparison Project Phase 5 (CMIP5) general
 764 circulation models used in this study

765

766

Model Name	Institution ID	Modeling Center
ACCESS1-0	CSIRO-BOM	Commonwealth Scientific and Industrial Research Organization (CSIRO) and Bureau of Meteorology (BOM), Australia
BCC-CSM1-1	BCC	Beijing Climate Center, China Meteorological Administration
CCSM4	NCAR	National Center for Atmospheric Research
CNRM-CM5	CNRM - CERFACS	Centre National de Recherches Météorologiques / Centre Européen de Recherche et Formation Avancée en Calcul Scientifique
GFDL-CM3	NOAA GFDL	NOAA Geophysical Fluid Dynamics Laboratory
GISS-E2-R	NASA GISS	NASA Goddard Institute for Space Studies
HadGEM2-AO	NIMR/KMA	National Institute of Meteorological Research/Korea Meteorological Administration
HadGEM2-CC	MOHC (additional realizations by INPE)	Met Office Hadley Centre (additional HadGEM2-ES realizations contributed by Instituto Nacional de Pesquisas Espaciais)
HadGEM2-ES	MOHC (additional realizations by INPE)	Met Office Hadley Centre (additional HadGEM2-ES realizations contributed by Instituto Nacional de Pesquisas Espaciais)
INM-CM4	INM	Institute for Numerical Mathematics
IPSL-CM5A-LR	IPSL	Institut Pierre-Simon Laplace
MIROC-ESM-CHEM	MIROC	Japan Agency for Marine-Earth Science and Technology, Atmosphere and Ocean Research Institute (The University of Tokyo), and National Institute for Environmental Studies
MIROC-ESM	MIROC	Japan Agency for Marine-Earth Science and Technology, Atmosphere and Ocean Research Institute (The University of Tokyo), and National Institute for Environmental Studies
MIROC5	MIROC	Atmosphere and Ocean Research Institute (The University of Tokyo), National Institute for Environmental Studies, and Japan Agency for Marine-Earth Science and Technology
MPI-ESM-LR	MPI-M	Max-Planck-Institut für Meteorologie (Max Planck Institute for Meteorology)
MRI-CGCM3	MRI	Meteorological Research Institute
NorESM1-M	NCC	Norwegian Climate Centre

767

768

769 **Table S3.** Predicted extent of forest, savanna and treeless areas in the tropical and subtropical
 770 Americas for 2070 under the RCP8.5 scenario for the 17 downscaled and calibrated CMIP5
 771 global climate models (GCM). Area in 10^3 km^2 . See description of climatic models in Table S2

772
 773

GCM	Forest	% Forest	Savanna	%Savanna	Treeless	% Treeless
ACCESS1-0	4562	21	14568	67	2717	12
BCC-CSM1-1	4942	23	14108	65	2797	13
CCSM4	4735	22	14343	66	2769	13
CNRM-CM5	4886	22	14384	66	2577	12
GFDL-CM3	3091	14	15707	72	3049	14
GISS-E2-R	4544	21	14313	66	2990	14
HadGEM2-AO	4011	18	15292	70	2543	12
HadGEM2-CC	3882	18	15289	70	2676	12
HadGEM2-ES	4127	19	14980	69	2740	13
INM-CM4	6107	28	12848	59	2891	13
IPSL-CM5A-LR	5668	26	13010	60	3168	15
MIROC-ESM-CHEM	5493	25	13551	62	2803	13
MIROC-ESM	6397	29	12632	58	2818	13
MIROC5	5057	23	13949	64	2841	13
MPI-ESM-LR	3355	15	15569	71	2923	13
MRI-CGCM3	5306	24	13928	64	2613	12
NorESM1-M	4767	22	14001	64	3079	14

774
 775
 776
 777
 778
 779
 780

781 **Table S4.** Predicted extent of the classes of the Forest-savanna transition index in the tropical
 782 and subtropical Americas for 2070 under the RCP8.5 scenario for the 17 downscaled and
 783 calibrated CMIP5 global climate models (GCM). This index is calculated as $p(\text{forest}) -$
 784 $p(\text{savanna})$. Values closer to 1 indicates cells with low uncertainty of being savanna, values
 785 closer to -1 indicates cells with low uncertainty of being forest and values closer to 0 indicates
 786 high uncertainty. Mean values are shown in Figure 6 (top). See description of climatic models in
 787 Table S2. Area in 10^3 km^2

788

789

GCM	(.5,1]	(.5,.4]	(.4,.3]	(.3,.2]	(.2,.1]	(.1,-.1]	(-.1,-.2]	(-.2,-.3]	(-.3,-.4]	(-.4,-.5]	(-.5,-1]
ACCESS1-0	6965	993	876	690	650	1288	663	657	716	721	1146
BCC-CSM1-1	6025	1000	962	840	678	1427	763	754	744	650	1286
CCSM4	6285	849	800	721	637	1388	661	709	620	737	1307
CNRM-CM5	6378	965	975	883	776	1598	773	681	643	797	1218
GFDL-CM3	6992	893	835	936	935	1928	760	616	291	157	331
GISS-E2-R	6890	883	854	729	635	1088	534	631	720	797	1347
HadGEM2-AO	7555	982	648	540	577	1171	554	540	623	707	997
HadGEM2-CC	7303	1099	795	653	666	1204	631	696	684	606	687
HadGEM2-ES	7364	1064	831	668	559	1239	680	689	673	739	717
INM-CM4	5940	771	651	538	488	1048	674	704	797	949	2440
IPSL-CM5A-LR	6514	689	532	540	551	1331	872	689	834	1111	1467
MIROC-ESM-CHEM	6252	933	766	629	609	1362	690	718	619	750	2014
MIROC-ESM	5423	880	759	725	723	1400	850	945	1065	1075	1744
MIROC5	6242	712	673	632	722	1401	821	822	744	697	1278
MPI-ESM-LR	7536	1288	1022	748	650	1121	579	531	459	582	643
MRI-CGCM3	6542	647	642	652	627	1366	807	906	816	726	1289
NorESM1-M	6191	859	801	680	646	1211	600	597	665	622	1692

790

791 **Table S5.** Predicted extent of the classes of the Savanna-Treeless transition index in the tropical
 792 and subtropical Americas for 2070 under the RCP8.5 scenario for the 17 downscaled and
 793 calibrated CMIP5 global climate models (GCM). This index is calculated as $p(\text{savanna}) -$
 794 $p(\text{treeless})$. Values closer to 1 indicates cells with low uncertainty of being treeless, values closer
 795 to -1 indicates cells with low uncertainty of being savanna and values closer to 0 indicates high
 796 uncertainty. Mean values are shown in Figure 6 (bottom). See description of climatic models in
 797 Table S2. Area in 10^3 km^2

798

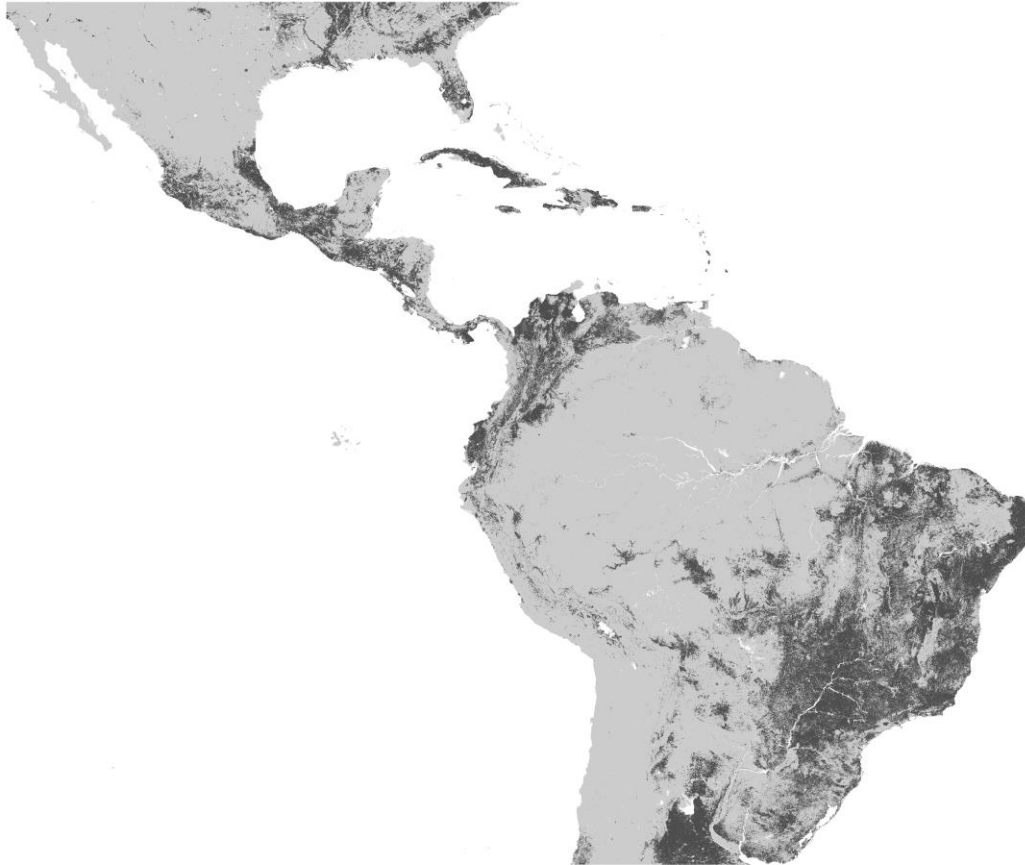
GCM	(.5,1]	(.5,.4]	(.4,.3]	(.3,.2]	(.2,.1]	(.1,-.1]	(-.1,-.2]	(-.2,-.3]	(-.3,-.4]	(-.4,-.5]	(-.5,-1]
ACCESS1-0	1694	217	225	205	198	350	197	248	276	354	2573
BCC-CSM1-1	1628	278	248	218	205	491	275	293	325	389	2440
CCSM4	1537	257	226	234	262	539	273	291	348	444	2788
CNRM-CM5	1483	268	230	218	203	362	206	255	292	347	2348
GFDL-CM3	1746	309	235	250	240	587	349	354	374	419	2369
GISS-E2-R	1856	254	207	207	226	497	233	230	276	333	2474
HadGEM2-AO	1495	238	213	196	192	446	268	301	356	430	2878
HadGEM2-CC	1547	269	240	240	203	381	242	278	345	405	2740
HadGEM2-ES	1692	258	246	214	171	336	205	253	273	396	2648
INM-CM4	1737	269	218	218	233	471	276	297	355	448	2373
IPSL-CM5A-LR	1990	290	260	236	206	402	221	251	326	375	2223
MIROC-ESM-CHEM	1791	245	220	206	184	357	223	248	300	348	2453
MIROC-ESM	1777	256	219	205	185	378	227	254	317	381	2130
MIROC5	1586	293	251	251	232	529	330	354	413	521	2404
MPI-ESM-LR	1846	262	220	197	211	366	185	250	369	411	2445
MRI-CGCM3	1475	211	222	255	235	468	289	356	407	531	2432
NorESM1-M	1856	272	227	231	257	485	243	293	324	435	2738

799

800

801 **Fig S1.** Distribution of areas undergoing human activities (categories 16-18 and 22 in the Global
802 Land Cover 2000 (GLC2000; Bartholome & Belward, 2005) in the Tropical and Subtropical
803 Americas (dark grey). These areas were filtered out from our analyses.

804



805

806

807 **REFERENCES**

808 Bartholome, E. & Belward, A. S. (2005) GLC2000: a new approach to global land cover mapping from
809 Earth observation data. *International Journal of Remote Sensing*, **26**, 1959-1977

810